

Passivation of irregular surfaces accessed by diffusion

M. Filoche^{*†‡}, D. S. Grebenkov[†], J. S. Andrade, Jr.[§], and B. Sapoval^{*†}

^{*}Physique de la Matière Condensée, Ecole Polytechnique, Centre National de la Recherche Scientifique, 91128 Palaiseau, France; [†]Centre de Mathématiques et de Leurs Applications, Ecole Normale Supérieure de Cachan, Centre National de la Recherche Scientifique, UniverSud, 61 Avenue du Président Wilson, F-94230 Cachan, France; and [§]Departamento de Física, Universidade Federal do Ceará, 60451-970 Fortaleza, Ceará, Brazil

Edited by H. Eugene Stanley, Boston University, Boston, MA, and approved January 22, 2008 (received for review August 1, 2007)

We investigate the process of progressive passivation of irregular surfaces accessed by diffusion. More precisely, we quantify through numerical simulations how the activity of the von Koch surface is gradually transferred from its initially active (or absorbing) regions to its less accessible regions. We show that in three dimensions, in sharp contrast with the two-dimensional case, the size of the successive active zones steadily decreases during the passivation process, even though a large quantity of alive surface remains available. As a consequence, in three dimensions, the evolution of the efficiency of a surface accessed by diffusion (i.e., by a Laplacian field) can exhibit long-tail behaviors that, unlike in two dimensions, strongly depend on its specific geometry. This fact has important implications for the design of heterogeneous catalysts under deactivation conditions, for the performance of heat exchangers subjected to passivation by “fouling,” and for changes in the behavior of the digestive system, where the activity of the absorbing intestinal membrane can be substantially affected by inflammatory disorders.

fractals | Laplace | deactivation | fouling

The passivation of surfaces working under diffusion-limited conditions is a general phenomenon that appears in many natural or industrial systems ranging from catalysis (1) to heat transfer (2), electrochemistry (3), and physiology (4). Although microscopically different, all of these processes share a single mathematical frame, namely the properties of the solutions of Laplace’s equation in a domain with irregular boundaries. In such situations, it is not only Laplacian screening that creates a strongly inhomogeneous active surface, but part of the surface activity may be progressively inhibited by phenomena bearing different names: passivation, fouling, poisoning, or restricted absorption, depending on the field. The cause for surface deterioration may be external, for example poisoning by an unwanted species or inflammation due to an external agent. It may be internal when the surface properties deteriorate because of its very activity. This is the case for parallel or serial fouling in catalysis.

In many of these situations, the surface is accessed by diffusion both for activity and deterioration. At the same time, large surface-to-volume ratios are needed to obtain enough macroscopic activity, which means that in all of these systems, very irregular or corrugated surfaces are present. This is the situation discussed here in a case where the surface is very irregular and the passivation is a direct consequence of the activity.

The performance of an interface accessed by diffusion is determined by the arrival probabilities on this interface. Quite surprisingly, very little is known about the distribution of the arrival probabilities of diffusing particles on a complex surface in three dimensions (5, 6), one of the reasons being the extreme difficulty of the numerical studies. The question of what defines the morphology of the “active” region is therefore mostly an open problem. Moreover, the effect of any passivation or poisoning phenomena will be to modify the physical properties of the surface, preventing the arriving particles from reacting and making them resume their diffusion in the surrounding bulk. The question of interest here is how the size of the region where most of the particles finally react or are absorbed will evolve, as

the passivation process gradually deactivates the initial alive interface. Let us first list a few examples where this issue is relevant.

In humans, as in other mammals, the transfer of nutrients from the digestive system to the blood is mostly realized in the small intestine in which the major transport mechanisms are passive diffusion and absorption (7). Moreover, the anatomy of the small intestine exhibits a fractal-like geometry, with finger-like structures at many different scales of magnification: flexures, plicae, villi, and microvilli (8). In this type of geometry, the most exposed parts of the intestinal membrane are easily accessed by diffusion and thus are the first to be altered by any inflammatory disorder or any chemical species that would diffuse in the digestive system. As a matter of fact, it is well known that a wide range of gastrointestinal disorders are associated with abnormal intestinal permeability (9).

Another important example of passivation is the phenomenon known as “fouling” (parallel or serial) in heterogeneous catalysis (10). During catalysis, this phenomenon consists in a secondary and parasitic reaction that passivates the catalyst in the regions that are active and eventually eliminates the entire activity of these regions. Laplacian screening in catalyst grains of very irregular geometry leads to active regions representing only a fraction of the total catalytic surface. The time evolution of the overall catalytic efficiency will then depend in a complex way on the accessibility of the more remote regions of the interface.

Diffusion also plays an important role in heat transfer. An enhanced efficiency of heat exchangers is most often achieved by building interfaces of very large surface, and fractal geometry is a good candidate for the design of such interfaces (11, 12). But the functioning of these interfaces can be substantially altered by a fouling process, namely the scale deposition, in which crystalline deposits of very low thermal conductivity locally reduce the heat transfer (13).

However, passivation is not always an unwanted phenomenon. For instance in electrochemistry, passivation is used to achieve a uniform deposition of copper atoms diffusing onto a rough surface. Once again, because of Laplacian screening, the region where most of the copper atoms arrive represents only a limited fraction of the total surface, which would normally lead to a nonuniform deposition (3). To avoid this, an inhibitor can be deposited on the first layer of copper atoms via an electrochemical reaction that is driven by an electric potential that also obeys Laplace’s equation. The inhibitor-clad region is then passivated for the deposition of copper atoms that can now reach into the holes of the rough surface (14).

In the steady-state regime, each of these systems shares the same mathematical frame in which there is a driving Laplacian

Author contributions: M.F., D.S.G., J.S.A., and B.S. designed research; D.S.G. performed research; M.F., D.S.G., J.S.A., and B.S. analyzed data; and M.F., D.S.G., J.S.A., and B.S. wrote the paper.

The authors declare no conflict of interest.

This article is a PNAS Direct Submission.

[†]To whom correspondence should be addressed. E-mail: marcel.filoche@polytechnique.edu.

© 2008 by The National Academy of Sciences of the USA

field in the bulk adjacent to an irregular reactive interface. Passivation, disease, aging, or fouling will likely start by damaging the most accessible and active part of the interface, so the question naturally arises: what happens after the initially active regions have been passivated? Here, we couch the answer for this question in terms of the catalytic problem. After deactivation, most of the diffusing particles hit a now passivated zone and are reflected, resuming their diffusion in the bulk to eventually react on an alive but deeper region of the catalytic surface. Consequently, regions that were initially poorly active become fully active until they are in turn passivated. This goes on and on until, finally, the whole catalytic interface is deactivated and the catalytic process stops. The question under scrutiny here is to determine and compare in two dimensions and three dimensions the evolution of the active zone, defined as the region of the interface in which “most” of the reaction occurs (15), and more precisely the evolution of its size.

In mathematical terms, the distribution of first arrival for Brownian particles onto a convoluted surface is called the “harmonic measure.” In two dimensions, a preliminary study (16) has shown that the size of the active zone remains almost constant throughout the passivation process, until the interface (which is in this case a corrugated line) is totally passivated. The argument for this result, first indicated by numerical simulations, is based on a conjectural extension of Makarov’s theorem (17, 18). For 2D Laplacian systems subject to Dirichlet boundary conditions, this theorem essentially states that whatever the shape (perimeter) of an interface, the size of the region where most of the activity takes place (the active zone) is of the order of the overall size L of the system.

The passivation process can be described as follows. At the beginning of the process, the alive sites are supposed to be uniformly distributed over the whole irregular surface. We suppose that the probability of reaction is equal to 1. This infinite reaction rate corresponds to a homogeneous Dirichlet boundary condition on the concentration of reactant molecules: $C = 0$. On such an interface, the activity, although existing in principle everywhere, is distributed in a very uneven manner because of Laplacian screening. One may then define an “active zone” as the smallest part of the interface carrying a given (large) fraction p of the activity. In this article, p will be arbitrarily chosen to be equal to 80%. Our results remain qualitatively valid for different values of p . The passivation process is then discretized and divided into the following steps (16).

- At first, the entire interface is alive. The distribution of arrival probabilities at the interface is calculated by a random-walk algorithm.
- The active region of the interface, which is only a fraction of the alive interface, is determined. The activity is in this case proportional to the harmonic measure density on the interface.
- This first active region is passivated. In mathematical terms, it would correspond to a particle concentration obeying Neumann boundary condition. Physically, it means that when a particle now hits a site belonging to this passivated region, it is reflected back and resumes its bulk diffusion until it reaches the regions that are still alive. In other words, this passivation process locally transforms a Dirichlet boundary condition into a Neumann boundary condition. The remaining alive interface thus consists in the former alive interface minus the newly passivated region.
- The new distribution of arrival probabilities is now computed using the new boundary condition (reflecting sites in the former active region).
- A new active region is determined, which is a subset of the remaining alive interface (the nonpassivated boundary). This new active region will be in turn passivated, and so on.

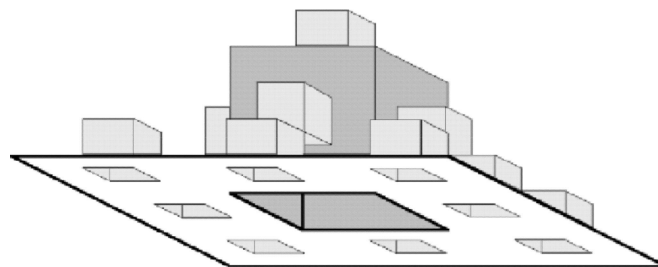


Fig. 1. Second generation of a prefractal surface based on the cubic Koch surface. The particles arrive from a distant source located far under the surface. The results presented in this study were computed up to the fifth-generation surface.

This passivation process thus generates at each iteration a new active region. All of these regions are different subsets of the interface. The whole interface can thus be decomposed as a sum of successive and disjoint active regions.

In what follows, we study the passivation of deterministic cubic Koch surfaces and quadratic Koch curves at different generations (Figs. 1 and 2). This particular choice does not reduce the generality of this work as randomness plays little role in the properties of diffusive transfer across irregular boundaries. Indeed, very different reactive interfaces accessed by diffusion, whether deterministic or random, reproduce almost the same response as long as their essential geometrical parameters (fractal dimension, width, and perimeter) are the same (19). This property plays a very important role because it can be used to generalize the results obtained for deterministic interfaces to disordered or random interfaces. As we show next, the choice of deterministic fractals also allowed us to develop and use an efficient technique (detailed in *Methods*) to compute the landing probabilities of random walkers onto a partially passivated deterministic fractal surface of fifth generation, which would have been almost impossible in the case of any disordered or random interface of comparable complexity.

Results

The combined use of two algorithms (described later in the article) has permitted us to study the passivation of a deterministic square Koch curve (two dimensions) up to the seventh generation and of a cubic Koch surface (three dimensions) up to the fifth generation, which is to our knowledge the most complex structure studied numerically until now for this type of problem.

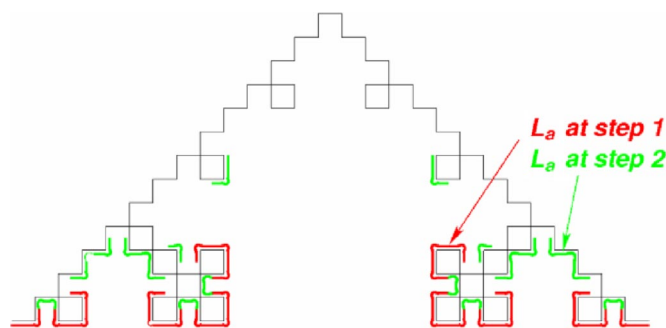


Fig. 2. Schematic view of the successive active then passivated regions. The diffusing particles are coming from below. The first active region is in red and has a length L_a . After the first step of the passivation process, the boundary condition on this region is set to Neumann, allowing a new region (in green) to become active. This region will be in turn passivated and so on, until the whole developed surface is passivated. In two dimensions, the active length L_a remains almost constant from one iteration to the next, until the entire surface is passivated.

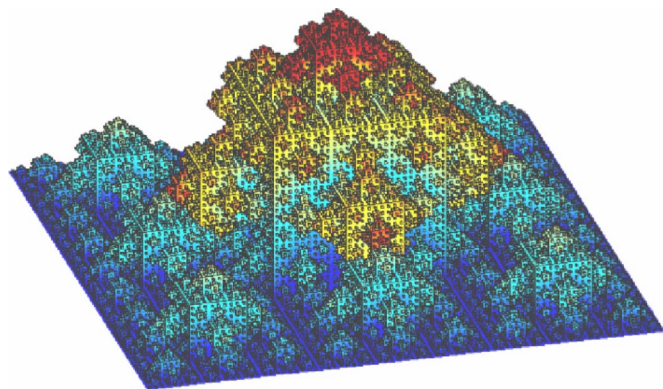


Fig. 3. Successive active regions during the passivation process of a fifth-generation prefractal surface based on the cubic Koch surface. Diffusing particles are coming from below and reach first mainly the blue region of the interface. Each color in the simulation represents a set of four successive passivated regions (dark blue corresponds to regions 1–4, light blue to 5–8, etc.). One can see that the size of the active region gradually decreases during the passivation process. At the end, only the dark-red regions on the tip are active.

One can take note visually of the complexity of the 3D surface and the evolution of the active zone in Fig. 3.

In two dimensions, the active region has approximately a constant length L_a at each step of the process, as schematically indicated in Fig. 2. As one can see in Fig. 4, this result is confirmed by numerical simulations for both the fourth and seventh generations. The observed oscillations can be attributed to the discrete scaling of the deterministic interface. Moreover, it is known from previous studies that the size of the active region is of the order of the width of the interface (16, 17). This implies that the number of passivation steps before the whole interface is deactivated should be of the order of the ratio between the total developed perimeter and the size of the interface. Quantitatively, the perimeter of the fourth generation (resp. seventh generation) of the quadratic Koch curve is ≈ 8 times (resp. 36 times) larger than the size of the system [more precisely, $(5/3)^4 \approx 7.7$ for the fourth generation and $(5/3)^7 \approx 35.7$ for the seventh generation]. Hence, one can see in Fig. 2 that the length of the active region becomes definitively smaller than 50% of the width of the cell after 8 and 37 passivation iterations, for the

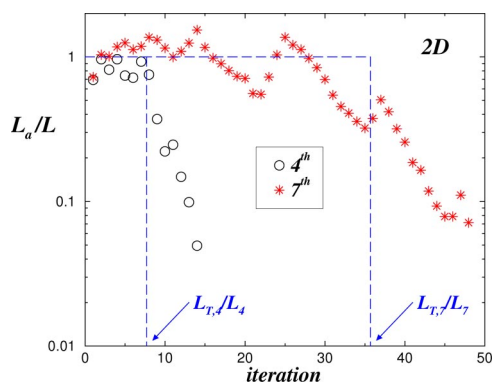


Fig. 4. Iterative deactivation for generations four and seven of 2D Koch curves. The size of the active region is plotted in units of the system width (L_4 or L_7) at each step of the passivation process. One can see that the normalized active length L_a/L remains almost constant throughout the process and is of the order of the structure width, until the number of iterations reaches the ratio between the perimeter of the interface and its width, L_T/L . These ratios are indicated by the vertical dashed lines. After this threshold, the passivation process rapidly terminates.

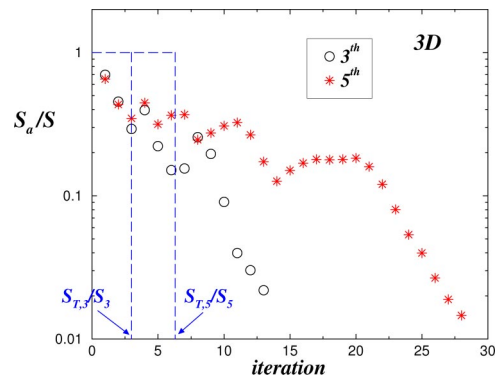


Fig. 5. Iterative deactivation for the third and fifth generations of the cubic Koch surface. The vertical axis represents the relative surface of the active region S_a (in units of the projected surface of the structure, resp. S_3 and S_5) at each step of the passivation process. In contrast with Fig. 4, the size of the active region at each step regularly decreases. It takes >25 steps to passivate almost the entire surface at of the fifth generation, whereas the total developed surface represents only 6 times the projected surface. The vertical lines correspond to the ratio of the total developed surface ($S_{T,3}$ and $S_{T,5}$) on the projected surface (S_3 and S_5). Note that the progressive slow decrease is very different from the 2D case.

fourth and seventh generations, respectively. After that, in both cases the size of the active region falls rapidly.

In three dimensions, the striking result is that, unlike in two dimensions, the surface of the active region S_a is not constant during the passivation process, but gradually decreases (as shown in Fig. 5 for $P = 80\%$). Even more, for the fifth generation, the developed surface in our 3D simulation contains ≈ 6 times the projected surface [$(13/9)^5 \approx 6.3$], but 25 passivation iterations are necessary to completely passivate the surface. We can observe from Figs. 4 and 5 that there is a net discrepancy between the 2D case and the 3D case: because of the properties of Brownian motion in two dimensions, the passivation process is much steadier than in three dimensions but stops much more abruptly. The 3D dynamics, in contrast, are characterized by a very slow decay of the size of the active zone.

To better distinguish the differences between 2D and 3D systems in a framework with reduced fluctuations, we also plot the evolution during the passivation process of two integral variables, namely the remaining alive length, $L_R(it) \equiv L_T - \sum_j^it_j$, and surface, $S_R(it) \equiv S_T - \sum_j^it_j$, for the 2D and 3D systems, respectively. Here, “ it ” is the iteration, L_T is the total perimeter (2D system), and S_T is the total surface (3D system) of the initial absorbing interfaces of the Koch structures.

The results shown in Fig. 6a indicate that the decay of L_R is approximately linear up to the eighth and thirtieth iteration for the fourth and seventh generations, respectively, of the Koch fractal curve. Moreover, this linear behavior in both cases follows very closely our theoretical prediction (the dashed lines in Fig. 6a) based on the conjectural extension of the Makarov’s theorem (16). This is analogous to saying that the size of the region passivated at each step is of the order of the interface width in two dimensions, which leads to the linear decay $L_R(it) \approx L_T - itL$. Fig. 6a Inset also shows that the initial decrease in L_R (before the first oscillation in the case of the seventh-generation Koch curve, due to the discreteness in its scaling) is compatible with a linear type of relationship.

The passivation process follows a rather different pathway in three dimensions. As shown in Fig. 6b, the decrease in the remaining alive surfaces S_R for the third and fifth generations of the fractal Koch surface clearly does not obey the corresponding constant decay law for a 3D system, namely $S_R(it) \approx S_T - itS$ (dashed lines in Fig. 6b). In addition, Fig. 6b Inset shows that S_R

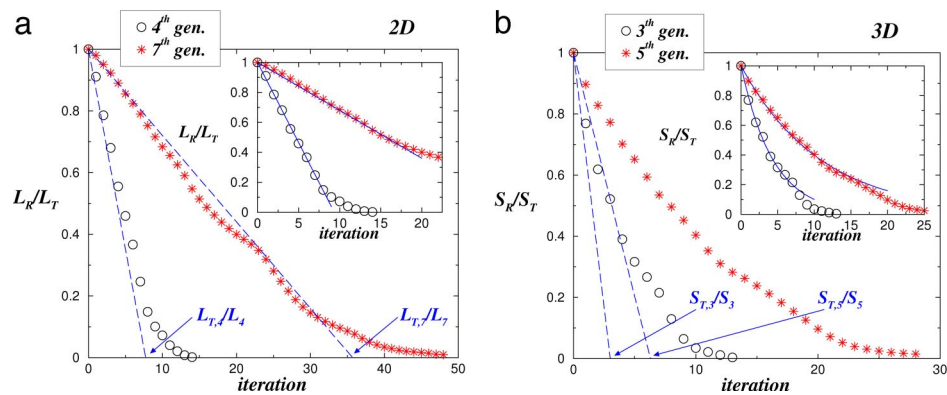


Fig. 6. Passivation decay in two and three dimensions. (a) Decay during the passivation process of the ratio between the remaining alive length and the initial total perimeter, L_R/L_T , for the fourth and seventh generations of the quadratic Koch curves. The dashed lines correspond to the theoretical prediction in which, at each iteration, the size of the passivated region is assumed to be equal to the width of the interface, namely $L_R(it) \approx L_T - itL$. (Inset) The initial decrease can be very well fitted by a linear relation, $L_R/L_T = 1 - ait$, with $a = 0.11$ and 0.032 for the fourth- and seventh-generation cases, respectively. (b) Decay of the ratio between the remaining alive and initial surfaces, S_R/S_T , for the third and fifth generations of the Koch fractal geometry. One can clearly see that the dashed lines corresponding to the constant decay law $S_R(it) \approx S_T - itS$ cannot describe the simulation results of the 3D system. Also in contrast with the linear behavior observed for the 2D case, *Inset* shows that the initial decrease of S_R/S_T follows an exponential behavior, $S_R/S_T = \exp(-bit)$, with $b = 0.23$ and 0.092 for the third and fifth generations, respectively.

decreases exponentially at the beginning of the passivation process for both third- and fifth-generation surfaces, in sharp contrast with the results from 2D simulations. At this point one should add, however, that here the iteration steps do not directly represent the real time. A more thorough analysis of the dynamics of this process in three dimensions remains an open problem (22).

These observations are significant, for example in the case of catalysis. On the one hand, the necessity of a large surface within a finite volume implies the use of very irregular surfaces. On the other hand, in three dimensions, the diffusion admittance of a region of typical size L scales as $(D \times L)$, whereas it is constant in two dimensions. As a consequence, the deep parts of the surface become more and more difficult to reach as the passivated zone increases and the random walkers are more and more prone to come back to the source. In consequence, the yield of reaction may decrease despite the fact that active regions still exist. In other words, for example, catalyst grains with very irregular internal porous geometry, even when they seem to be exhausted, may still contain a large amount of alive surface. Put simply, the diffusion process does not allow the reactant particles to reach efficiently the deep regions of the catalyst. In this case, a large amount of catalyst can be wasted just because it is not easily accessed by 3D diffusion anymore. From this point of view, an engineered (2D + 1) geometry (with translational invariance) would be preferable.

These results may also cast a new light on very different systems in which diffusion plays a significant role. In the lung of mammals, the alveolar membrane, a complex surface embedded within the chest, is mostly accessed by diffusion. In some pulmonary diseases that affect this membrane, the local decrease of the membrane permeability would produce an effect similar to passivation (23). The results presented here tend to show that, in this case, not only might the gas transfer occur in a more distal region of the lung, but the size of the active surface that contributes effectively to the gas transfer could also be reduced, leading to a further decrease of the diffusing lung capacity.

In conclusion, by taking advantage of a new numerical algorithm (using the partially passivated boundary as an effective source for reactive particles), we have been able to compute in three dimensions the iterative passivation for high-generation orders of the cubic Koch surface. In our study, this type of surface is used as an example of a highly irregular geometry. In

significant contrast with the 2D case, for which a mathematical argument permits an understanding of the evolution of the active region, it has been shown that, in three dimensions, the size of the active zone steadily decreases during the passivation process. This leads to a longer tail of low activity that involves a large portion of the sites. These results should have direct implications for the understanding of the dynamics of complex diffusive systems in nature.

Methods

Classical numerical techniques such as finite differences or finite elements have strong limitations in terms of mesh size and computation time for solving the Laplace equation near complex boundaries. For instance, if each elementary square of the cubic Koch surface is meshed with only 5 nodes on each side, more than 9 million nodes ($5 \times 5 \times 13^5$) are needed to mesh the surface at the fifth generation. This would lead to a bulk mesh of at least several hundreds of million nodes. To overcome this difficulty, a Monte Carlo approach has been used where the harmonic measure on the boundary is computed by launching random walkers from a distant source and monitoring their arrival sites on the surface. Moreover, here we use a fast random walk algorithm (20) that, in the case of deterministic interfaces, can be greatly improved by taking advantage of the exact scaling of the structure (21). In this algorithm, the length of each step of the Brownian trajectory of a particle diffusing toward the Koch surface is not constant but equal to the current distance between the particle and the surface. The value of this distance, normally lengthy to compute, can be found simply in the case of a deterministic self-similar structure such as the Koch surface. The particle is considered to have hit the boundary when it approaches the Koch surface at a distance smaller than a given threshold. For a large enough number of particles, the distribution of their arrivals on the surface reproduces the harmonic measure and the distribution of the activity.

Although this “geometry adapted fast random walk” algorithm (GAFRW) has proved to be very efficient, its direct application to a partially passivated boundary is still not sufficient to solve the problem here. The reason is the following: after a few iterations of the passivation process, the remaining alive regions are highly screened. So a reactant particle launched from a distant source has to follow a very long stochastic trajectory, with a large number of reflections on the passivated sites of the boundary, before reaching any potentially active region. The extremely large computational time required for further passivation iterations makes it then difficult or even impossible to study the whole passivation process.

This difficulty has been overcome here by using the distribution of the activity at step n as the initial source distribution for the next step ($n + 1$). As a matter of fact, the distribution of the activity at step ($n + 1$) is composed of two types of particles: (i) particles arriving directly on the nonpassivated part of the boundary (corresponding to its contribution to the initial harmonic measure) and (ii) particles arriving after being reflected by the already passivated part of the boundary up to step n . The distant source of diffusing

particles is thus replaced by a fictitious source on the boundary itself. Because the last passivated regions are close to the remaining alive zones, using them as sources considerably enhances the efficiency of the computation. The following formalism develops this idea into a rigorous mathematical frame.

If one considers the bulk domain called Ω and its boundary $\partial\Omega$, one can define an operator T^A that will "transfer" by Brownian motion a distribution f defined on the subset A of $\partial\Omega$ onto the complementary subset $(\partial\Omega - A)$ by

$$T^A f \equiv \frac{\partial u}{\partial n} \Big|_{\partial\Omega - A}, \quad [1]$$

where u is the solution of the system

$$\begin{cases} \Delta u = 0 & \text{in } \Omega \\ \frac{\partial u}{\partial n} = f & \text{on } A \\ u = 0 & \text{on } \partial\Omega - A. \end{cases} \quad [2]$$

In physical terms, if f corresponds to a distribution of particles arriving on A , then $T^A f$ is the distribution of the same particles arriving on $\partial\Omega - A$, after they have been reflected on A and have resumed their diffusion in Ω .

If one now considers two disjoint subsets A_1 and A_2 (which correspond to two successive passivated regions), one can compute the distribution $T^{(A_1 \cup A_2)} f$ by successively applying the operators T^{A_1} and T^{A_2} : the function u , namely the solution of System 2 for $T^{(A_1 \cup A_2)}$, can be written as $u_1 + u_2$ where

$$\begin{cases} \Delta u_1 = 0, \Delta u_2 = 0 & \text{in } \Omega \\ \frac{\partial u_1}{\partial n} = f, \frac{\partial u_2}{\partial n} = 0 & \text{on } A_1 \\ u_1 = 0, \frac{\partial u_2}{\partial n} = f - \frac{\partial u_1}{\partial n} & \text{on } A_2 \\ u_1 = u_2 = 0 & \text{on } \partial\Omega - (A_1 \cup A_2). \end{cases} \quad [3]$$

It is easy to check that u does indeed satisfy System 2. From that point, the function $[T^{(A_1 \cup A_2)} f]$ can be written in $(\partial\Omega - (A_1 \cup A_2))$ as the sum of the two contributions of u_1 and u_2 :

$$T^{A_1 \cup A_2} f = \frac{\partial u_1}{\partial n} + \frac{\partial u_2}{\partial n} = T^{A_1} f + T^{(A_1 \cup A_2)} f|_{A_2} - T^{(A_1 \cup A_2)}(T^{A_1} f)|_{A_2}. \quad [4]$$

This equation simply states that the distribution of particles that react on the surface when both A_1 and A_2 are passivated is constituted of

1. the particles that would have reacted at the same position, even if only A_1 was passivated (term $T^{A_1} f$).
2. the particles that come first to A_2 (they would have reacted here if only A_1 was passivated) and that are now reflected since A_2 is also passivated (term $T^{(A_1 \cup A_2)} f|_{A_2}$).
3. the particles that would have been first reflected by A_1 , and then sent to A_2 . These are now also reflected by A_2 and sent back to react further in the nonpassivated part of the surface (term $T^{(A_1 \cup A_2)}(T^{A_1} f)|_{A_2}$). There is a minus sign in front of the third term because the current density of particles coming from A_1 to A_2 is reflected and sent back, which corresponds in fact to a positive contribution.

ACKNOWLEDGMENTS. For financial support of this work, we thank the Brazilian agencies Coordenação de Aperfeiçoamento de Pessoal de Nível Superior, Conselho Nacional de Desenvolvimento Científico e Tecnológico, Fundação Cearense de Apoio ao Desenvolvimento Científico e Tecnológico, and Financiadora de Estudos e Projetos; the French agency Comité Français d'Evaluation de la Coopération Universitaire et Scientifique avec le Brésil; and the Agence Nationale de la Recherche (Project 05-SEST-001).

1. Froment GF, Bischoff KB (1980) *Chemical Reactor Analysis and Design* (Wiley, New York).
2. Epstein N (1988) in *Fouling Science and Technology, Proceedings of the NATO Advanced Study Institute on Advances in Fouling Science and Technology, 1987*, eds Melo LF, Bernardo CA (Kluwer Academic, Dordrecht, The Netherlands), p 15.
3. Pricer TJ, Kushner MJ, Alkire RC (2002) Monte Carlo simulation of the electrodeposition of copper. II. Acid sulfate solution with blocking additive. *J Electrochem Soc* 149:C406–C412.
4. Weibel ER (1984) *The Pathway for Oxygen* (Harvard Univ Press, Cambridge, MA), pp 265–266.
5. Bourgain J (1987) On the Hausdorff dimension of harmonic measure in higher dimension. *Invent Math* 87:477–483.
6. Wolff T (1995) *Essays on Fourier analysis in honor of Elias M. Stein*, Princeton Mathematical Series, ed Wainger S (Princeton Univ Press, Princeton), Vol 42, pp 321–384.
7. DeSesso JM, Jacobson CF (2001) Anatomical and physiological parameters affecting gastrointestinal absorption in humans and rats. *Food Chem Toxicol* 39:209–228.
8. Yan RG, Yan GZ, Yang BH (2005) Fractal analysis on human colonic pressure activities based on the box-counting method. *Int J Inf Technol* 2:226–228.
9. Farhadi A, Banan A, Fields J, Keshavarzian A (2003) Intestinal barrier: An interface between health and disease. *J Gastroenterol Hepatol* 18:479–497.
10. Bartholomew CH (2001) Mechanisms of catalyst deactivation. *Appl Catal A Gen* 212:17–60.
11. Andrade JS, Jr, Henrique EAA, Almeida MP, Costa MHAS (2004) Heat transport through rough channels. *Physica A* 339:296–310.
12. Meyer JP, Van der Vyver H (2005) Heat transfer characteristics of a quadratic Koch island fractal heat exchanger. *Heat Transer Eng* 26:22–29.
13. Helalizadeh A, Müller-Steinhagen H, Jamialahmadi M (2006) Application of fractal theory for characterisation of crystalline deposits. *Chem Eng Sci* 61:2069–2078.
14. Shingubara S, et al. (2004) Bottom-up fill of copper in deep submicrometer holes by electroless plating. *Electrochem Solid-State Lett* 7:C78–C80.
15. Sapoval B (1994) General formulation of Laplacian transfer across irregular surfaces. *Phys Rev Lett* 73:3314–3316.
16. Sapoval B, Costa MHAS, Andrade JS, Jr, Filoche M (2004) Laplacian transport towards partially passivated 2D irregular interfaces: A conjectural extension of the Makarov theorem. *Fractals* 12:381–387.
17. Makarov NG (1985) On the distortion of boundary sets under conformal mappings. *Proc London Math Soc* 51:369–384.
18. Jones PW, Wolff TH (1988) Hausdorff dimension of harmonic measures in the plane. *Acta Math* 161:131–144.
19. Filoche M, Sapoval B (2000) Transfer across random versus deterministic fractal interfaces. *Phys Rev Lett* 84:5776–5779.
20. Meakin P (1985) The structure of two-dimensional Witten-Sander aggregates. *J Phys A* 18:L661–L666.
21. Grebenkov DS, Lebedev AA, Filoche M, Sapoval B (2005) Multifractal properties of the harmonic measure on Koch boundaries in two and three dimensions. *Phys Rev E* 71:056121.
22. Filoche M, Sapoval B, Andrade JS, Jr (2005) Deactivation dynamics of rough catalytic surfaces. *Am Inst Chem Eng J* 51:998–1008.
23. Sapoval B, Filoche M, Weibel ER (2002) Smaller is better—but not too small: A physical scale for the design of the mammalian pulmonary acinus. *Proc Natl Acad Sci USA* 99:10411–10416.